European Journal of Pharmacology 623 (2009) 65–72

Contents lists available at ScienceDirect

European Journal of Pharmacology

journal homepage: www.elsevier.com/locate/ejphar

Neuropharmacology and Analgesia

Differential activation of spinal microglial and astroglial cells in a mouse model of peripheral neuropathic pain

Joanna Mika [a], Maria Osikowicz [a], Ewelina Rojewska [a], Michal Korostynski [b], Agnieszka Wawrzczak-Bargiela [b], Ryszard Przewlocki [b], Barbara Przewlocka [a,*]

[a] Department of Pain Pharmacology, Institute of Pharmacology, Polish Academy of Sciences, 12 Smetna Street, 31-343 Krakow, Poland
[b] Department of Molecular Neuropharmacology, Institute of Pharmacology, Polish Academy of Sciences, 12 Smetna Street, 31-343 Krakow, Poland

ARTICLE INFO

Article history:
Received 6 August 2009
Accepted 9 September 2009
Available online 17 September 2009

Keywords:
Neuropathic pain
Glia
C1q
CD11b/c
OX42
GFAP

ABSTRACT

The pharmacological attenuation of glial activation represents a novel approach for controlling neuropathic pain, but the role of microglial and astroglial cells is not well established. To better understand the potential role of two types of glial cells, microglia and astrocytes, in the pathogenesis of neuropathic pain, we examined markers associated with them by quantitative RT-PCR, western blot and immunohistochemical analyses in the dorsal horn of the lumbar spinal cord 7 days after chronic constriction injury (CCI) to the sciatic nerve in mice. The mRNA and protein of microglial cells were labeled with C1q and OX42(CD11b/c), respectively. The mRNA and protein of astrocytes were labeled with GFAP. The RT-PCR results indicated an increase in C1q mRNA that was more pronounced than the increased expression of GFAP mRNA ipsilateral to the injury in the dorsal spinal cord. Similarly, western blot and immunohistochemical analyses demonstrated an ipsilateral upregulation of OX42-positive cells (72 and 20%, respectively) and no or little (8% upregulation) change in GFAP-positive cells in the ipsilateral dorsal lumbar spinal cord. We also found that chronic intraperitoneal injection of the minocycline (microglial inhibitor) and pentoxifylline (cytokine inhibitor) attenuated CCI-induced activation of microglia, and both, but not fluorocitrate (astroglial inhibitor), diminished neuropathic pain symptoms and tactile and cold sensitivity. Our findings indicate that spinal microglia are more activated than astrocytes in peripheral injury-induced neuropathic pain. These findings implicate a glial regulation of the pain response and suggest that pharmacologically targeting microglia could effectively prevent clinical pain syndromes in programmed and/or anticipated injury.

1. Introduction

Accumulating evidence suggests that at the level of the spinal cord, glial cells and the molecules they produce play an important role in the development and maintenance of persistent pain (Griffin et al., 2007; Gwak and Hulsebosch 2009; Ledeboer et al., 2005; Levin et al., 2008; Mika et al., 2009; Rodriguez Parkitna et al., 2006; Watkins et al., 2001, 2005). Glial cells dynamically modulate the function of neurons under both physiological and pathological conditions (Temburni and Jacob, 2001). Recently, some authors have suggested that astroglial and neuronal functions can be dynamically modulated by microglia cells, which are implicated in the initiation phase of injury-induced pain (Colburn et al., 1999; DeLeo et al., 2004; Jin et al., 2003; Narita et al., 2006). Microglia cells become activated immediately after injury and via ion and electrical changes in the neuronal/glial microenvironment, which induces hypersensitivity and leads to further enhancement of glial activation (DeLeo et al., 2004). Numerous models of neuropathic pain have indicated that microglia can influence development of this phenomenon, e.g., partial sciatic nerve ligation (Coyle, 1998), spinal nerve ligation (Jin et al., 2003) and spinal cord injury (Gwak and Hulsebosch, 2009, Hains and Waxman, 2006; Popovich et al., 1997). The activation of astrocytes, which are thought to contribute to the maintenance of chronic pain (Raghavendra et al., 2004; Tanga et al., 2004), is delayed following spinal cord injury. Spinal astroglia activities have been intensively studied after spinal cord injury (Gwak and Hulsebosch 2009, Hains and Waxman, 2006; Popovich et al., 1997), whereas little is known about their role in pain after peripheral injury (Obata et al., 2006; Xu et al., 2007b).

Despite the numerous studies, the type of glial cell that plays the key role in the pathomechanism of peripheral nerve injury-induced neuropathic pain remains unclear. This is very important from the therapeutic point of view, since neuroimmune alterations contribute to pathological changes in many insufficiently treated neurodegenerative disorders. To study the potential involvement of different glial cells in the initiation and maintenance of neuropathic pain, we compared nerve injury-induced activation of microglia and astroglia after administration of drugs that modulate activation of various types of glial cells. Minocycline, a potent inhibitor of microglial activation and proliferation (Amin et al., 1996;

* Corresponding author. Tel.: +48 12 6623398; fax: +48 12 6374500.
E-mail address: przebar@if-pan.krakow.pl (B. Przewlocka).

0014-2999/$ – see front matter © 2009 Elsevier B.V. All rights reserved.
doi:10.1016/j.ejphar.2009.09.030

Aronson, 1980; Colovic and Caccia, 2003; Tikka et al., 2001), pentoxifylline, a non-specific cytokine inhibitor and an inhibitor of phosphodiesterase (Liu et al., 2007; Lundblad et al., 1995; Neuner et al., 1994) and fluorocitrate, which acts as general astroglial inhibitor that disrupts astroglial metabolism by blocking aconitase (Willoughby et al., 2003) were employed. To identify the involvement of glial cell subtypes in CCI-induced neuropathic pain, we studied how glial inhibitors with different mechanisms of action influence injury-induced changes in mRNA and protein expression of glia activation markers in the spinal cord. Additionally, we investigated their influence on neuropathic pain symptoms such as tactile and cold sensitivity.

2. Materials and methods

2.1. Animals

Male Albino-Swiss mice (20–25 g) from Charles River Laboratories International, Inc. (Germany) were housed in cages lined with sawdust under standard 12/12 h light/dark cycle (lights on at 08:00 h) with food and water available ad libitum. All experiments were performed according to the recommendations of IASP (Zimmermann, 1983) and the NIH Guide for Care and Use of Laboratory Animals and were approved by the local Bioethics Committee (Cracow, Poland).

2.2. Surgical preparations

Chronic constriction injury (CCI) was produced by loosely tying three ligatures (4/0 silk) around the sciatic nerve under sodium pentobarbital anesthesia (60 mg/kg; i.p.). The biceps femoris and the gluteus superficial were separated, and the right sciatic nerve was exposed. The ligatures (4/0 silk) were tied loosely around the nerve distal to the sciatic notch with 1 mm spacing until a brief twitch in the respective hind limb was observed as previously described (Bennett and Xie, 1988). After surgery, all mice developed long-lasting neuropathic pain symptoms measured by tactile and cold sensitivity.

2.3. Drugs

Chemicals and their sources were as follows: minocycline hydrochloride (Sigma, USA), pentoxifylline (Polfilin, Polfarma, Poland), and fluorocitrate (fluorocitric acid; Sigma, USA). All drugs were dissolved in sterile water. The highest possible doses that were safe and well tolerated of minocycline (60 μmol/kg), pentoxifylline (70 μmol/kg) and fluorocitrate (0.2 μmol/kg) were used. The drugs were administered intraperitoneally first at 16 h and 30 min before CCI and then twice daily for 7 days as previously described (Raghavendra et al., 2003; Mika et al., 2007). This administration schedule was used because systemic minocycline attenuates the activation of microglia more efficiently when the inhibitor is injected before injury (Raghavendra et al., 2003; Ledeboer et al., 2005). The control groups received a vehicle injection (i.p.) according to the same schedule. The behavioral tests were conducted on day 7 after CCI 30 min and following drug administration. Tissue from all mice was collected 7 days after CCI and 4 h after drug or vehicle administration for RT-PCR, western blot and immunohistochemical analyses.

2.4. Antibodies and probes

Antibodies for western blot (rabbit polyclonal anti-OX42 (anti-CD11 (b/c)) and the rabbit polyclonal anti-GFAP antibody were purchased from Novus Biologicals, Inc. For immunohistochemistry, primary antibodies rat anti-mouse OX42 (CD11b/c-microglia marker; 1:500 dilution) and mouse anti-glial fibrillary acidic protein (GFAP-astrocyte marker, 1:2000) were purchased from BD Biosciences, USA and Chemicon International, Germany, respectively. The following TaqMan primers (Applied Biosystems, Foster, CA, USA) and probes were used: Mm00432142_m1 (C1q; mouse complement component 1, q subcomponent, beta polypeptide); Mm01253033_m1 (GFAP; mouse glial fibrillary acidic protein); Mn00446968_m1 (HPRT; mouse hypoxanthine guanine phosphoribosyl transferase).

2.5. Behavioral tests

2.5.1. Tactile sensitivity (von Frey test)

Mechanical sensitivity to stimuli was measured using a set of calibrated nylon monofilaments (Stoelting, USA). Approximately 3 days before CCI, naive mice were placed in transparent plastic experimental cages with a wire mesh floor. After 5 min, mice were tested with von Frey filaments for adaptation. None of the mice responded to filaments from 0.6 to 6 g. During the experiment, mice that had undergone CCI were habituated to the experimental cage for 5 min before testing. Increasing strengths of von Frey filaments were applied sequentially to the plantar surface of the hind paw of each mouse. The intensity of mechanical stimulation was increased from 0.6 to 6 g in a graded manner using successively larger filaments until the hind paw was withdrawn. The general procedure was based on the paper by Chaplan et al. (1994) that demonstrated how to employ von Frey filaments in rats. We then modified our measurements according to the study described by Sommer and Schafers (1998).

2.5.2. Cold sensitivity (cold plate test)

Cold sensitivity was assessed using the cold plate test (Cold/Hot Plate Analgesia Meter No.05044 Columbus Instruments, USA) according to Choi et al. (1994) and Jasmin et al. (1998). The temperature of the cold plate was kept at 2 °C and the cut-off latency was 30 s. The mice were acclimated to the cold plate apparatus 3 days before CCI. During acclimation, none of the mice responded to the cold over the 30 s period. For the experiments, mice were placed on the cold plate apparatus and the time until the hind paw was lifted was recorded. In all cases, the injured paw was the first to react. Mice were immediately removed from the cold plate apparatus after a reaction was observed.

2.6. Biochemical tests

2.6.1. Analysis of gene expression by qPCR

The lumbar (L5–L6) region of the spinal cord was removed and divided into ipsilateral and contralateral parts with respect to the side of injury immediately after the sacrifice of the mice 7 and 17 days after CCI. The tissue samples were placed in individual tubes with the tissue storage reagent RNAlater (Qiagen Inc., Valencia, CA, USA), frozen on dry ice and stored at −20 °C until RNA isolation. Samples were thawed at room temperature and homogenized in 1 ml of Trizol reagent (Invitrogen, Carlsbad, CA, USA). RNA concentration was measured using a NanoDrop ND-1000 Spectrometer (NanoDrop Technologies). RNA quality was determined by chip-based capillary electrophoresis using a RNA 6000 Nano LabChip Kit and Agilent Bioanalyzer 2100 (Agilent), according to the manufacturer's instructions. Reverse transcription was performed using Omniscript reverse transcriptase (Qiagen Inc., Valencia, CA, USA) at 37 °C for 60 min. RT reactions were carried out in the presence of an RNAse inhibitor (rRNAsin, Promega, USA) and oligo(dT16) primer (Qiagen Inc., Valencia, CA, USA). cDNA was diluted 1:8 with H_2O, and for each reaction ~50 ng of cDNA synthesised from total RNA template from individual animals was used. Quantitative real-time RT-PCR (qPCR) reactions were performed using Assay-On-Demand Taqman probes, according to the manufacturer's protocol (Applied Biosystems, Foster, CA, USA), and run on an iCycler device (BioRad, Hercules, CA, USA). For each assay, control reactions without RT enzyme were performed to exclude the contribution of contaminating genomic DNA. The amplification efficiency for each assay was determined by running a standard dilution curve. We analyzed changes in the transcription of complement component C1q (C1q; microglia marker; Schafer et al., 2000) and glial fibrillary acidic protein (GFAP; astroglial marker; Tanga et al., 2004). The following TaqMan primers and probes were used: Mm00432142_m1

(mouse complement component 1, q subcomponent, beta polypeptide); Mm01253033_m1 (mouse glial fibrillary acidic protein); Mn00446968_m1 (mouse hypoxanthine guanine phosphoribosyl transferase), Mm00446968_m1 (mouse hypoxanthine guanine phosphoribosyl transferase). HPRT did not significantly change in mouse CCI models, and therefore served as an adequate housekeeping gene (data not shown). The cycle threshold values were calculated automatically by iCycler IQ 3.0 software using default parameters. RNA abundance was calculated as $2^{-(\text{threshold cycle})}$. The expression of hypoxanthine guanine phosphoribosyl transferase transcript was quantified to control for variations in cDNA amounts.

2.6.2. Western blot

The lumbar (L5–L6) region of the spinal cord was removed and divided into ipsilateral and contralateral parts with respect to the side of injury or left and right in the case of naive mice. Tissue samples were homogenized in RIPA buffer and cleared by centrifugation (10,000 ×*g* for 10 min). The protein concentration in the supernatant was determined using the BCA Protein Assay Kit (Sigma). Samples containing 30 µg of protein were heated for 8 min at 99 °C in loading buffer (50 mM Tris–HCl, 2% SDS, 2% β-mercaptoethanol, 8% glycerol and 0.1% bromophenol blue) and resolved by SDS-PAGE on 12% polyacrylamide gels. After gel electrophoresis, proteins were electrophoretically transferred to nitrocellulose membranes (Trans-Blot; Bio-Rad). The blots were blocked using 5% blocking buffer (2.5% albumin + 2.5% non-fat dry milk) in TBST (Tris-buffered saline with 0.1% Tween 20) for 1 h. The rabbit polyclonal anti-OX42 (anti-CD11 (b/c)) was used against the type 3 complement receptor to detect positive microglial cells. The OX42(CD11b/c) antigen is commonly used as a microglial marker in nervous tissue (Perry et al., 1993; Robinson et al., 1986). Blots were incubated with rabbit polyclonal anti-OX42(CD11b/c) at a 1:300 dilution (Novus Biologicals, Inc). A rabbit polyclonal anti-GFAP antibody (1:5000 dilution) (Novus Biologicals, Inc) was used to detect GFAP positive astroglia (Coyle, 1998). Blots were incubated overnight at 4 °C with primary antibodies and then incubated with a peroxidase-conjugated secondary antibody (goat anti-rabbit IgG, Vector) at a dilution of 1:1000 for 1 h at room temperature. After three 10 min washes in TBS and 0.1% Tween-20 and one wash in TBS, immunocomplexes were detected using a buffered solution of 250 mM luminal sodium salt and 30% hydrogen peroxidase in 1 M Tris–HCl (pH 8.5) containing 90 mM p-coumaric acid and visualized using a Fujifilm LAS-1000 fluorimager system. The blots were stripped and reprobed with a mouse antibody against β-actin (1:5000, Sigma Aldrich) as a loading control. Relative levels of immunoreactivity were quantified using the Fujifilm Image Gauge software.

2.6.3. Immunohistochemistry

Seven days after CCI, mice were deeply anesthetized with pentobarbital (60 mg/kg; i.p.) and perfused transcardially with saline (0.9% NaCl) followed by ice-cold fixative (4% paraformaldehyde in 0.1 M phosphate buffer, pH 7.4). Spinal cords were removed and were post-fixed with the same fixative for 2 h and placed in 10% sucrose in phosphate buffer, followed by 20% and 30% sucrose until the tissue sank. The spinal cord L2–L6 segments were embedded in Jung tissue-freezing medium (Leica) and cut on a cryostat. Transverse sections (40 µm thick) were collected free-floating in PBS (pH 7.4) for immunolabeling. The sections were washed in PBS with 0.2% Triton X-100, pH 7.4 (PBS + T), incubated in a solution of 0.3% H_2O_2 in water for 30 min to quench endogenous peroxidase activity, washed extensively in PBS + T and incubated with 3% normal serum in PBS + T for 30 min to reduce non-specific staining. The sections were subsequently incubated overnight at 4 °C with rat anti-mouse OX42 (CD11b/c-microglia marker; 1:500, BD Biosciences, USA) and mouse anti-glial fibrillary acidic protein (GFAP-astrocyte marker, 1:2000, Chemicon International, Germany). The sections were then rinsed in PBS + T and incubated for 1 h at room temperature with secondary biotinylated antibodies from the ABC kits (Vector Laboratories). After extensive washings with PBS + T, these sections were incubated for 1 h with AB complex containing an avidin–HRP conjugate and then washed again with PBS + T. The secondary antigen was visualized with 3,3-diaminobenzidine tetrahydrochloride (DAB, Sigma). The reaction was terminated by addition of extensive PBS + T and by subsequent PBS washings. The sections were then mounted on gelatin-subbed slides, dehydrated in ascending alcohol concentrations, cleared through xylene and covered with DPX resin.

The immunohistochemistry DAB staining is a valuable tool to for qualitative and quantitative analysis of protein level (Garrison et al., 1991; Ma and Quirion, 2002; Xin et al., 2009). Immunohistochemistry allows to follow changes of segmental and laminar distribution of glial responses and enables their detection even when limited to small areas. To optimize reproducibility, we rigorously kept the conditions of tissue processing, development of the reaction and conditions of illumination during image collection. Changes in the ipsilateral and contralateral spinal cord from CCI mice were compared to those of naïve mice. For densitometry, four to five sections per animal were selected that showed the best match to the L5–L6 lumbar segments illustrated in the stereotaxic atlas (Paxinos and Watson, 1986). The immunostained regions were outlined manually and the intensity of immunohistochemical signal, expressed in gray scale units, was measured with the aid of a computer-assisted image analysis system consisting of a Nikon Eclipse 80i microscope equipped with an x/y/z movement-sensitive stage and a monochromatic CCD camera (Evolution VF; Media Cybernetics, Inc., Silver Spring, MD, USA). The Image ProPlus 4.0 (UK) digitizer and software and the Scion software (NIH, Frederick, MD, USA) were used for the analysis. Gray levels were measured by subtracting the gray level of the background in a region outside the section from the specific signal measured over the section surface. Astroglial and microglial response, measured by evaluation of GFAP and OX42 immunostaining, was analyzed throughout the whole gray matter of the ipsi- and contralateral sides of each section and measured changes of segmental and laminar (I–IV) distribution.

2.7. Data analysis

The behavioral data are presented as a percentage of control (naive mice) ± S.E.M. of 10–16 mice per group. The results of the experiments were evaluated by one-way analysis of variance (ANOVA). The differences between groups were further analyzed by Bonferroni post-hoc test. $^{*}p<0.001$ indicates a significant difference vs. control (contralateral paw of CCI-exposed mice). The behavioral results of the pharmacological treatment are presented as % of control (mean ± S.E.M.; 8–12 mice per group). Inter-group differences were analyzed by an ANOVA followed by Bonferroni's Multiple Comparison Test ($^{***}p<0.001$ indicates a significant difference between vehicle-treated naive and vehicle-treated CCI-exposed mice; $^{\#\#}p<0.01$ and $^{\#\#\#}p<0.001$ indicates a significant difference compared to vehicle-treated CCI-exposed mice). For the quantitative real-time PCR analysis, the data are presented as the fold change of control (naive mice) mean ± S.E.M., which represents the normalized averages derived from the threshold cycles in the qPCR of six to eight ipsilateral and contralateral samples (i.e., six to eight mice per group). The inter-group differences were analyzed by ANOVA followed by Bonferroni's Multiple Comparison Test ($^{*}p<0.05$ and $^{***}p<0.001$ indicates that statistical analysis was performed between the ipsilateral and contralateral sides; $^{o}p<0.05$ indicates that statistical analysis was performed vs. day 7). The western blot and immunohistochemistry results are presented as a percentage of control (naive mice) from the densitometry analysis. Values are shown as the mean of 10–18 samples from 5–10 mice per group ± S.E.M. Inter-group differences were analyzed by ANOVA followed by Bonferroni's Multiple Comparison Test ($^{*}p<0.05$ and $^{***}p<0.001$ indicates a significant difference between vehicle-treated naïve and vehicle-treated CCI-exposed mice; $^{\#}p<0.05$,

##$p<0.001$ and ###$p<0.001$ indicates a significant difference compared to vehicle-treated CCI-exposed mice).

3. Results

3.1. Development of neuropathic pain symptoms

All mice with CCI of the sciatic nerve developed neuropathic pain symptoms as shown by the von Frey test (Fig. 1A) and cold plate test (Fig. 1B). Tactile hypersensitivity was observed on the ipsilateral paw from day 3 until day 21. Following CCI on day 7 (when the tissue was collected for biochemical evaluation) the ipsilateral paw responded to a stimulation of 1.2 ± 0.2 g, while the contralateral paw responded to 5.5 ± 0.2 g. The difference of reaction was significant (Fig. 1A). The strongest cold hypersensitivity was observed between days 3 and 17. On the seventh day after CCI, the ipsilateral paw responded to cold stimulus after 5.4 ± 0.8 s and a significant difference versus the reaction of contralateral paw (29.5 ± 0.2 s) was measured. Strong cold hypersensitivity persisted until day 17, followed by a slow decline over time (Fig. 1B).

3.2. Quantification of C1q and GFAP transcript expression in the lumbar spinal cord 7 and 17 days after CCI

In the ipsilateral spinal cord, a significant upregulation of C1q mRNA (Fig. 2A) and GFAP mRNA (Fig. 2B) expressions was observed compared to the contralateral side 7 days after CCI. Our RT-PCR analysis indicated that 17 days after CCI, the level of C1q mRNA significantly decreased, and GFAP mRNA returned to the control level. Expression of HPRT, a housekeeping gene, was measured in all samples as a control. There was no statistically significant difference in HPRT mRNA levels between the ipsilateral and contralateral sides of the spinal cord after CCI (data not shown).

3.3. The influence of minocycline, pentoxifylline and fluorocitrate on CCI-induced changes in behavior on day 7 after injury in mice

Mice were injected with either the microglial inhibitor minocycline (60 µmol/kg; i.p.), the phosphodiesterase inhibitor pentoxifylline (70 µmol/kg; i.p.) or the astroglial inhibitor fluorocitrate (0.2 µmol/kg; i.p.) preemptively (16 h and 30 min) before CCI and then twice daily over 7 days (Fig. 3). Administration of minocycline and pentoxifylline attenuated mechanical (Fig. 3A) and cold (Fig. 3B) hypersensitivity when measured 7 days after CCI. Administration of the astroglial inhibitor fluorocitrate (0.2 µmol/kg; i.p.), however, did not influence mechanical sensitivity (0.7 ± 0.04 g vs. 0.9 ± 0.06 g) or cold hyperalgesia

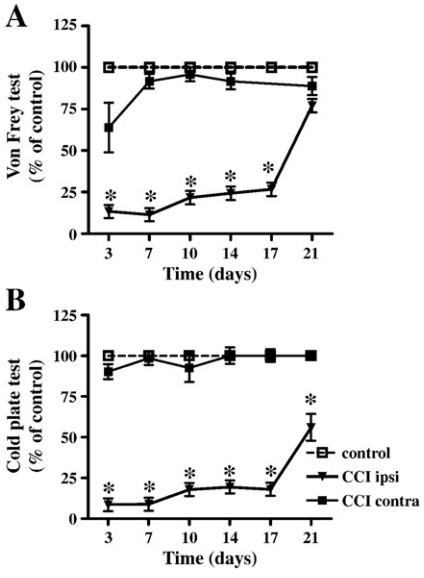

Fig. 1. The mechanical (A, mice; von Frey test) and cold sensitivity (B, mice; cold plate test) was measured 3–21 days after chronic constriction injury (CCI) to the sciatic nerve. On day 7 post-CCI, the ipsilateral paw responded to a stimulation of 1.2 ± 0.2 g as measured by von Frey test and of 5.4 ± 0.8 s as measured by cold plate test. The data are presented as % of control ± S.E.M. (10–16 mice per group). Inter-group differences were analyzed by Bonferroni's Multiple Comparison Test. *$p<0.001$ indicates a significant difference compared to the contralateral paw of CCI-exposed mice.

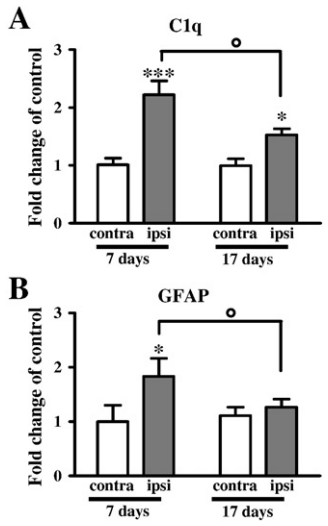

Fig. 2. Quantitative real-time PCR analysis of C1q (A) and GFAP (B) gene expression in the ipsilateral and contralateral lumbar (L5–L6) spinal cords 7 and 17 days after chronic constriction injury (CCI) in mice. The data are presented as fold change of control (naïve mice) mean ± S.E.M., which represent normalized averages derived from the threshold cycles in qPCR six to eight ipsilateral and contralateral samples (i.e., six to eight mice for each group. The inter-group differences were analyzed by an ANOVA followed by Bonferroni's Multiple Comparison Test. *$p<0.05$, ***$p<0.001$ indicates the statistical analysis was performed between the ipsilateral and contralateral sides. °$p<0.05$ indicates the statistical analysis was performed vs. day 7.

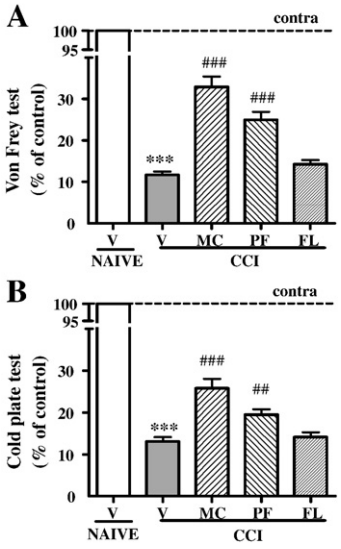

Fig. 3. The effect of vehicle (V), minocycline (MC; 60 µmol/kg), pentoxifylline (PF; 70 µmol/kg) and fluorocitrate (0.2 µmol/kg) intraperitoneally administered 16 h and 30 min before CCI and then for 7 days twice daily on mechanical (A; von Frey test) and cold sensitivities (B; cold plate test) measured 7 days after CCI. Results are presented as % of control (mean ± S.E.M.; 8–12 mice per group). Mechanical and cold sensitivities were assessed 30 min after drug or vehicle administration. Inter-group differences were analyzed by an ANOVA followed by Bonferroni's Multiple Comparison Test. ***$p<0.001$ indicates a significant difference between vehicle-treated naïve and vehicle-treated CCI-exposed mice; ##$p<0.01$ and ###$p<0.001$ indicate a significant difference compared to vehicle-treated CCI-exposed mice. The dotted line shows the results obtained on contralateral side.

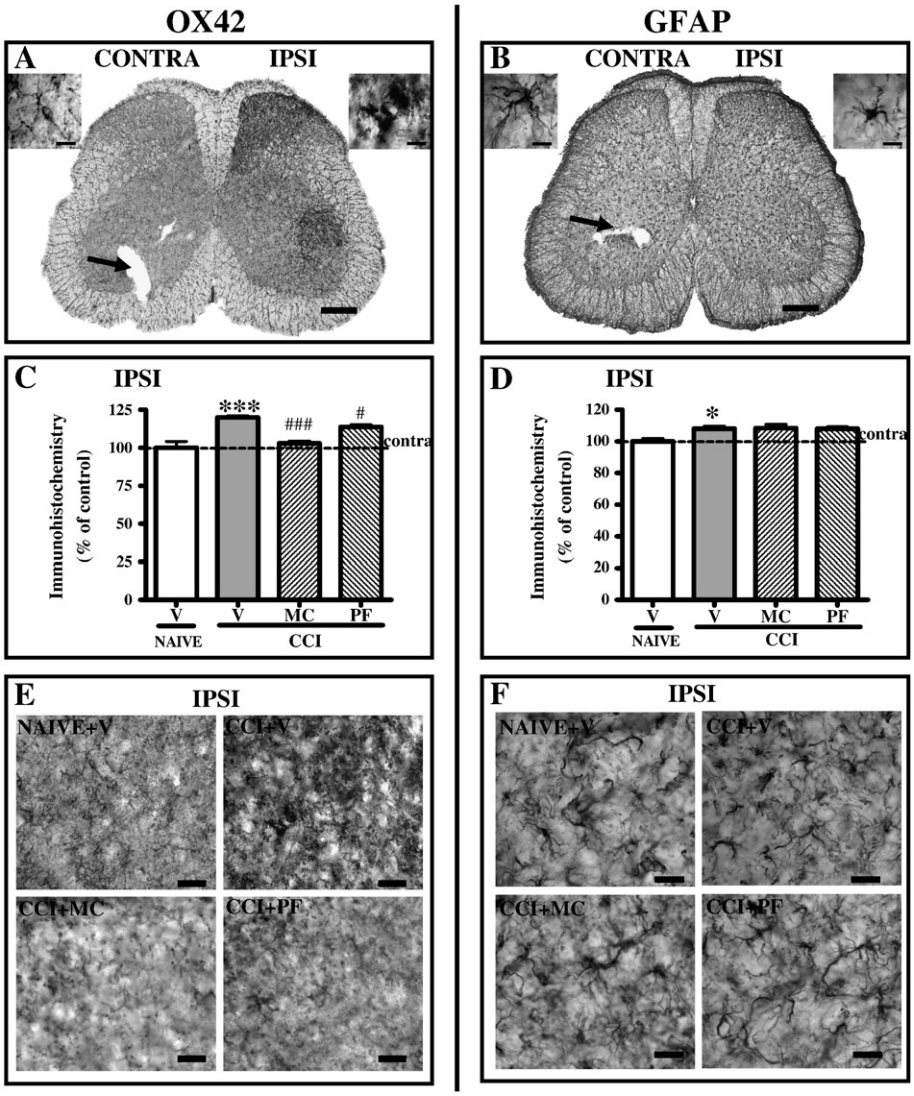

Fig. 4. The immunohistochemical photographs show at low magnification (5×) the OX42 (CD11b/c, A) and GFAP (B) proteins in the ipsilateral and contralateral (marked with arrow) lumbar (L5–L6) spinal cords 7 days after CCI in mice. The inset in A shows a higher magnification (100×) of microglia cells. The left inset shows the typical resting microglial morphology, and the right inset illustrates the enlarged and amoeboid morphological features of activated microglia cell bodies. The insets in B shows higher magnification (100×) of the typical astroglial morphology of long slender processes and small soma diameter. Scale bar = 250 μm, inset = 25 μm. The results of immunohistochemical analysis of OX42(CD11b/c; C) and GFAP (D) protein levels measured in the ipsilateral lumbar (L5–L6) spinal cord after chronic intraperitoneal treatment of vehicle (V), minocycline (MC; 60 μmol/kg) and pentoxifylline (PF; 70 μmol/kg) on day 7 after CCI in mice. Values are shown as the mean of 10–18 samples from five to seven mice per group ± S.E.M. Results are presented as a percentage of control (vehicle-treated naive mice) of the densitometry analysis of all sections. Inter-group differences were analyzed by an ANOVA followed by Bonferroni's Multiple Comparison Test. *$p<0.05$ and ***$p<0.001$ indicates a significant difference between vehicle-treated naïve and vehicle-treated CCI-exposed mice. #$p<0.05$ and ###$p<0.01$ indicate a significant difference compared to vehicle-treated CCI-exposed mice. The dotted line shows the results obtained on the contralateral side. The immunohistochemical photographs of OX42(CD11b/c; E) and GFAP (F) protein show the changes in the ipsilateral lumbar spinal cord under high magnification (63×) in CCI + V, CCI + MC and CCI + PF groups compared to naive + V. Scale bar = 25 μm.

(3.9 ± 0.3 s vs. 4.2 vs. 0.3 s) at this time point. This inhibitor was therefore not used for subsequent biochemical analysis.

3.4. The influence of minocycline, pentoxifylline and fluorocitrate on OX42 and GFAP protein levels in the lumbar spinal cord 7 days after CCI

Antibodies against OX42 revealed moderate expression of resident microglia in the contralateral side of the spinal cord (Fig. 4A), exhibiting a quiescent or resting type morphology (left inset; Fig. 4A). The photographs of representative immunohistochemical results at low magnification (5×; Fig. 4A) performed 7 days after CCI showed that on the ipsilateral side of the lumbar spinal cord, the expression of OX42 (microglia marker) protein was noticeably elevated in comparison to the contralateral spinal cord. The upper left inset of Fig. 4A (higher magnification; 100×) illustrates a typical resting microglial cell on the contralateral side, whereas the upper right inset shows enlarged and amoeboid-activated microglia cells on the ipsilateral side. The OX42 immunoreactive cells with typical morphology of microglia increased both in number and staining intensity in the ipsilateral dorsal horn (Fig. 4A, E). The western blot performed 7 days after CCI revealed that on the ipsilateral side of the lumbar spinal cord, the expression of OX42 protein was noticeably elevated in comparison to the contralateral side (Fig. 5A). Compared to control animals (naïve mice), injury significantly enhanced the protein expression of the spinal microglia marker OX42 on the ipsilateral side (72%) (Fig. 5A). The elevation of OX42 in vehicle-treated CCI-exposed mice was decreased in mice that had preemptively and repeatedly received minocycline and pentoxifylline (36% and 17%, respectively; Fig. 5A). Similar significant effects were observed by immunohistochemical analysis (Fig. 4C). The ipsilateral increase of C1q mRNA (Fig. 2A) was paralleled by an equal increase in OX42 protein as measured by immunohistochemistry (Fig. 4A, C, E) as well as western blot (Fig. 5A) at 7 days after CCI.

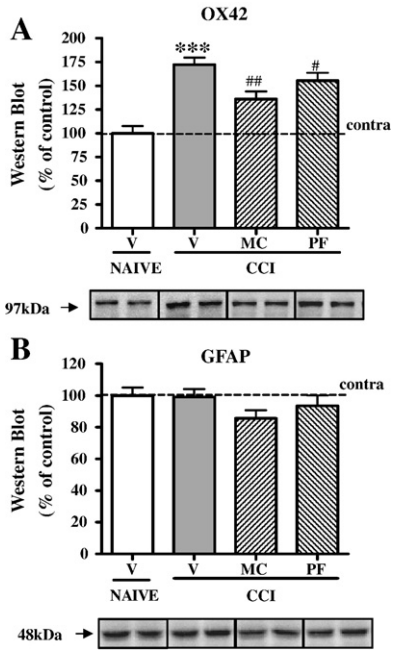

Fig. 5. Western blot analysis of OX42 (CD11b/c; A) and GFAP (B) protein levels measured in the ipsilateral lumbar (L5–L6) spinal cord after chronic intraperitoneal treatment of vehicle (V), minocycline (MC; 60 μmol/kg) and pentoxifylline (PF; 70 μmol/kg) on day 7 after CCI in mice. Values are shown as the mean of 10–18 samples from 5–10 mice per group ± S.E.M. Results are presented as a % of control (vehicle-treated naïve mice) densitometry analysis of all sections. Inter-group differences were analyzed by an ANOVA followed by Bonferroni's Multiple Comparison Test. ***$p<0.001$ indicates a significant difference between vehicle-treated naive and vehicle-treated CCI-exposed mice. #$p<0.05$ and ##$p<0.01$ indicate a significant difference compared to vehicle-treated CCI-exposed mice. The dotted line shows the results obtained on contralateral side.

The photographs of representative immunohistochemical results at low magnification (5×) clearly show the astroglial characteristics of GFAP-positive cells (Fig. 4B). Immunohistochemistry for detection of GFAP, a marker for normal as well as reactive astroglia, revealed that in naive and contralateral side of the spinal cords from CCI-exposed mice showed a baseline expression of GFAP (Fig. 4B, D, and F). The GFAP-positive astroglia showed round nuclei with fibers of different lengths that were arranged in a rather regular radial pattern and were distributed uniformly throughout the spinal cord sections. Higher magnification (100×; Fig. 4B insets) shows cells with typical astroglial morphology of long slender processes and small soma diameter. The immunohistochemical analysis revealed only upregulation of the astroglial protein marker GFAP (Fig. 4D) 7 days after CCI compared to naive animals and the contralateral side. The elevation of 8.1% of GFAP in vehicle-treated CCI-exposed mice was not decreased in mice that had preemptively and repeatedly received minocycline and pentoxifylline (8.5% and 8.1%, respectively; Fig. 4D). The regulation of GFAP was not detected by western blot (Fig. 5B). No significant changes in the astroglial marker GFAP were detected by western blot in CCI-exposed or drug-treated CCI-exposed mice when compared to naïve mice (Fig. 5B).

4. Discussion

It has previously been shown that glia can strongly influence synaptic communication between neurons and lead to pathological pain (Haydon, 2001; Marchand et al., 2005; Milligan et al., 2003; Watkins and Maier, 2003). Early studies demonstrated a role of glia in regulating neuropathic pain symptoms. The role of particular types of glial cells in pain regulation, however, remains to be elucidated. In the present study, we found that microglia are predominantly and profoundly activated ipsilaterally in the dorsal horn of the lumbar spinal cord after CCI to the sciatic nerve in mice. Preemptive and chronic intraperitoneal injections of minocycline, which selectively inhibits the activation of microglia (Cui et al., 2008; Hains and Waxman, 2006), and pentoxifylline, which inhibits cytokine release (Lundblad et al., 1995; Neuner et al., 1994; Raghavendra et al., 2003, 2004; Wie et al., 2009; Zabel et al., 1993), attenuated CCI-induced activation of microglia. Moreover, both inhibitors diminished neuropathic pain symptoms and tactile and cold sensitivity, which develop due to abnormal neuronal activity associated with injury to the peripheral nerve (Mika et al., 2007; Zimmermann, 2001). Using RT-PCR, immunohistochemistry and western blot analyses, we also found that activation of astroglia is much less pronounced in this CCI model of neuropathic pain. In contrast, many papers have described an increase of astrocyte activation using other models of spinal cord injury. The reason for this is that with injuries to the central nervous system, the described changes are directly in a place of damage. This supports our results of low astrocyte activation observed in the CCI model of peripheral nerve injury, where the changes in the spinal cord are secondary and distant from the place of injury and reflect the complexity of nerve response to injury. Because of this, spinal astroglia were not strongly activated in our experiments, results that are in contrast to previous studies using other spinal cord injury models that found very high astroglia activation (Gwak and Hulsebosch 2009, Hains and Waxman, 2006; Obata et al., 2006; Popovich et al., 1997). Another reason for the differences in the activation of microglia and astroglia cells in various models of neuropathic pain could come from the time-course of their activation after different types of injury. Popovich et al. (1997) has shown that activation of microglial and astroglial cells after spinal cord injury begins as early as 12 h and lasts up to 28 days. The peak of microglial activation was observed 3–7 days post-injury, similar to our model, but astrocytes were more prominent at later survival times (7–28 days). The time course of glia cell activation is different after peripheral injury to the sciatic nerve. Our previously obtained results, which are in agreement with others (Obata et al., 2006; Xu et al., 2007a), showed that the microglial activation begins 2 days after CCI and is most pronounced 7–9 days afterwards. This was followed by a slow decrease in both neuropathic pain symptoms and microglia activation (17–21 days after CCI). We and others (Obata et al., 2006; Xu et al., 2007b) have found that the most pronounced increase of astroglia activation in the mouse spinal cord after CCI occurs on day 7, and the alterations returned to the control level on days 14–17. The seventh day was therefore chosen in the current study for comparison of the effects of different glial inhibitors. This was the only possible time point when the activation of microglial and astroglial cells occurred after CCI. These results indicate that microglia activation is the key factor that contributes to neuronal hyper-responsiveness and alterations in behavior related to neuropathic pain in the early stages following CCI. The present study aimed to identify the type of glia cell that is essential to the initiation and/or maintenance of the changes leading to neuropathy after peripheral injury by comparing the effectiveness of three drugs (minocycline, pentoxifylline and fluorocitrate) that modulate the activity of different types of glial cells.

Pentoxifylline is the most frequently used inhibitor of CCI-induced activation of microglia, and has been shown to significantly attenuate formalin-induced pain and CCI-induced neuropathic pain in rats (Dorazil-Dudzik et al., 2004; Mika et al., 2007, 2009), and postoperative pain in patients (Lu et al., 2004; Wordliczek et al., 2000). Using behavioral studies, we and others have shown restoration of the analgesic activity of morphine by propentofylline or pentoxifylline treatment in neuropathic pain models (Lundblad et al., 1995; Mika et al., 2007; Neuner et al., 1994; Raghavendra et al., 2003, 2004; Sweitzer et al., 2001; Tawfik and DeLeo, 2007). Similarly, Gwak and Hulsebosch (2009) have shown that spinal cord injury-induced neuropathic pain was attenuated by propentofylline. In the present study, we observed that intraperitoneal administration of pentoxifylline effectively attenuated tactile and cold sensitivity in parallel to reducing microglial cell activation. By blocking the release of proinflammatory cytokines and consequently diminishing microglia activation, pentoxifylline administered before a scheduled surgery is a viable strategy for preventing the

development of postoperative pain (Lu et al., 2004; Wordliczek et al., 2000).

In contrast to cytokine inhibitors, neuropathic pain symptoms in our model were not attenuated by the astroglial inhibitor fluorocitrate. Nevertheless, our results are not in contrast to other studies (Chen et al., 2007, Lan et al., 2007; Nakagawa et al., 2007; Obata et al., 2006; Qin et al., 2006) that have described the attenuation of pain symptoms by fluorocitrate. Its effect was demonstrated in models with high astrocyte activation, which is not the case in our study. In our CCI model, we demonstrated only a slight upregulation of GFAP mRNA and protein on day 7, which decreased to the control level by day 17. These findings, consistent with those of Xu et al. (2007b), suggest that inhibition of astrocytes could be important for maintenance of neuropathic pain, but that targeting microglia could be a promising approach to preventing the development of neuropathic pain.

The most pronounced inhibition of injury-induced behavioral and biochemical alterations were observed in the present study after preemptive and repeated treatment with minocycline, which selectively inhibits the activation of microglia (Cui et al., 2008; Mika et al., 2009). However, (Gieseler et al., 2009; Mishra et al., 2009) have shown that minocycline can influence neurons in cultures, but no evidence from *in vivo* studies. Minocycline, by reducing the activation of microglial cells, reduces the expression of pain mediators like cytokines, chemokines, neurotransmitters, prostaglandins (Ledeboer et al., 2005; Mika et al., 2009; Raghavendra et al., 2003; Strassburger et al., 2008; Zhang et al., 2006; Yrjänheikki et al., 1999). Recently, Cui et al. (2008) found that the analgesic effect of minocycline under neuropathic pain conditions is associated with a direct reduction of p38MAPK, which was found to be activated after injury in spinal cells by labeling them with the microglial marker OX42, but not in NeuN-expressing neurons or GFAP-expressing astrocytes. Similar to our results, Hains and Waxman (2006) showed using a different neuropathic pain model that minocycline rapidly attenuated hypersensitivity of spinal neurons by a decrease in the level of phosphorylated p38 in microglia. There are also early reports from human therapy studies showing that minocycline is safe and clinically well tolerated in the treatment of neurodegenerative disorders (Blum et al., 2004; Smith and Leyden, 2005); however, minocycline has not been used for the treatment of neuropathic pain. In addition, given its ease passage through the blood-brain barrier, low incidence of adverse effects in clinical studies and effectiveness in a number of animal models of neurological disease, minocycline is emerging as a promising candidate in pain therapy (Yong et al., 2004). Minocycline also has neuroprotective properties (Fehlings and Baptiste, 2005; Lin et al., 2007; Sterling et al., 2004) and it enhances morphine's effectiveness and delays the development of morphine tolerance by attenuating microglia activation in naïve and CCI-exposed mice (Mika et al., 2007, 2009).

An understanding of the molecular mechanisms that underlie the effects of microglia on pain processing should lead to the development of new and more efficient approaches for the treatment of pain. Additionally, modulation of microglial cells and, in consequence, neuroimmune responses have the potential to increase the efficiency of drugs such as morphine during neuropathic pain therapy, as was also shown in our previous study (Cui et al., 2008; Mika et al., 2009, Tawfik and DeLeo, 2007). There are also early clinical studies that provide strong support for the suggestion that minocycline and pentoxifylline are safe and effective in clinical use and could be potentially useful agents to diminish pain symptoms and enhance the effects of morphine under pathological pain conditions (Blum et al., 2004; Lu et al., 2004; Wordliczek et al., 2000). A major challenge to the development of new drug strategies for the treatment of neuropathic pain is specifically targeting the pathological actions of proinflammatory cytokines and chemokines released by microglia in the spinal cord. Our results suggest that targeting microglia activation by administration of minocycline may effectively prevent the possible development of persistent postoperative pain after a scheduled surgical intervention and/or potentiate the effects of antinociceptive drugs in neuropathic pain therapy.

Acknowledgements

This research was supported by the statutory funds and by grant (N N405 375937) from the Ministry of Science and Higher Education. The authors are grateful to Profs. Julita Czarkowska-Bauch, Malgorzata Skup and Krzysztof Wedzony for valuable help in the analysis of the immunohistochemical results and photographs.

References

Amin, A.R., Attur, M.G., Thakker, G.D., 1996. A novel mechanism of action of tetracyclines: effects on nitric oxide synthases. Proc. Natl. Acad. Sci. U.S.A. 93, 14014–14019.
Aronson, A.L., 1980. Pharmacotherapeutics of the newer tetracyclines. J. Am. Vet. Med. Assoc. 176, 1061–1068.
Bennett, G.J., Xie, Y., 1988. A peripheral mononeuropathy in rat that produces disorders of pain sensation like those seen in man. Pain 33, 87–107.
Blum, D., Chtarto, A., Tenenbaum, L., Brotchi, J., Levivier, M., 2004. Clinical potential of minocycline for neurodegenerative disorders. Neurobiol. Dis. 17, 359–366.
Chaplan, S.R., Bach, F.W., Pogrel, J.W., Chung, J.M., Yaksh, T.L., 1994. Quantitative assessment of tactile allodynia in the rat paw. J. Neurosci. Methods 53, 55–63.
Chen, J., Zhang, J., Zhao, Y., Yuan, L., Nie, X., Li, J., Ma, Z., Zhang, Y., Wang, Q., Chen, Y., Jin, Y., Rao, Z., 2007. Hyperalgesia in response to traumatic occlusion and GFAP expression in rat correction of parabranchial nucleus: modulation with fluorocitrate. Cell Tissue Res. 329, 231–237.
Choi, Y., Yoon, Y.W., Na, H.S., Kim, S.H., Chung, J.M., 1994. Behavioral signs of ongoing pain and cold allodynia in a rat model of neuropathic pain. Pain 59, 369–376.
Colburn, R.W., Rickman, A.J., DeLeo, J.A., 1999. The effect of site and type of nerve injury on spinal glial activation and neuropathic pain behavior. Exp. Neurol. 157, 289–304.
Colovic, M., Caccia, S., 2003. Liquid chromatographic determination of minocycline in brain-to-plasma distribution studies in the rat. Life Sci. 791, 337–343.
Coyle, D.E., 1998. Partial peripheral nerve injury leads to activation of astroglia and microglia which parallels the development of allodynic behavior. Glia 23, 75–83.
Cui, Y., Liao, X.X., Liu, W., 2008. A novel role of minocycline: attenuating morphine antinociceptive tolerance by inhibition of p38 MAPK in the activated spinal microglia. Brain Behav. Immun. 22, 114–123.
DeLeo, J.A., Tanga, F.Y., Tawfik, V.L., 2004. Neuroimmune activation and neuroinflammation in chronic pain and opioid tolerance/hyperalgesia. Neuroscientist. 10, 40–52.
Dorazil-Dudzik, M., Mika, J., Schafer, M.K., Li, Y., Obara, I., Wordliczek, J., Przewłocka, B., 2004. The effects of local pentoxifylline and propentofylline treatment on formalin-induced pain and tumor necrosis factor-alpha messenger RNA levels in the inflamed tissue of the rat paw. Anesth. Analg. 98, 1566–1573.
Fehlings, M.G., Baptiste, D.C., 2005. Current status of clinical trials for acute spinal cord injury. Injury 36, 113–122.
Garrison, C.J., Dougherty, P.M., Kajander, K.C., Carlton, S.M., 1991. Staining of glial fibrillary acidic protein (GFAP) in lumbar spinal cord increases following a sciatic nerve constriction injury. Brain Res. 565, 1–7.
Gieseler, A., Schulze, A.T., Kupach, K., Haroon, M.F., Wolf, G., Siemen, D., Kreutzmann, P., 2009. Inhibitory modulation of the mitochondrial permeability transition by minocycline. Biochem Pharmacol. 77, 888–896.
Griffin, R.S., Costigan, M., Brenner, G.J., Ma, C., Scholz, J., Moss, A., Allchorne, A.J., Stahl, G.L., Woolf, C.J., 2007. Complement induction in spinal cord microglia results in anaphylatoxin C5a-mediated pain hypersensitivity. J. Neurosci. 27, 8699–8708.
Gwak, Y.S., Hulsebosch, C.E., 2009. Remote astrocytic and microglial activation modulates neuronal hyperexcitability and below-level neuropathic pain after spinal injury in rat. Neuroscience 161, 895–903.
Hains, B.C., Waxman, S.G., 2006. Activated microglia contribute to the maintenance of chronic pain after spinal cord injury. J Neurosci. 26, 4308–4317.
Haydon, P.G., 2001. GLIA: listening and talking to the synapse. Nat. Rev. Neurosci. 2, 185–193. Review.
Jasmin, L., Kohan, L., Franssen, M., Janni, G., Goff, J.R., 1998. The cold plate as a test of nociceptive behaviors: description and application to the study of chronic neuropathic and inflammatory pain models. Pain 75, 367–382.
Jin, S.X., Zhuang, Z.Y., Woolf, C.J., Ji, R.R., 2003. p38 mitogen-activated protein kinase is activated after a spinal nerve ligation in spinal cord microglia and dorsal root ganglion neurons and contributes to the generation of neuropathic pain. J. Neurosci. 23, 4017–4022.
Lan, L., Yuan, H., Duan, L., Cao, R., Gao, B., Shen, J., Xiong, Y., Chen, L.W., Rao, Z.R., 2007. Blocking the glial function suppresses subcutaneous formalin-induced nociceptive behavior in the rat. Neurosci Res. 57, 112–119.
Ledeboer, A., Sloane, E.M., Milligan, E.D., Frank, M.G., Mahony, J.H., Maier, S.F., Watkins, L.R., 2005. Minocycline attenuates mechanical allodynia and proinflammatory cytokine expression in rat models of pain facilitation. Pain 115, 71–83.
Levin, M.E., Jin, J.G., Ji, R.R., Tong, J., Pomonis, J.D., Lavery, D.J., Miller, S.W., Chiang, L.W., 2008. Complement activation in the peripheral nervous system following the spinal nerve ligation model of neuropathic pain. Pain 137, 182–201.
Lin, C.S., Tsaur, M.L., Chen, C.C., Wang, T.Y., Lin, C.F., Lai, Y.L., Hsu, T.C., Pan, Y.Y., Yang, C.H., Cheng, J.K., 2007. Chronic intrathecal infusion of minocycline prevents the development of spinal-nerve ligation-induced pain in rats. Reg Anesth Pain Med. 32, 209–216.
Liu, J., Feng, X., Yu, M., Xie, W., Zhao, X., Li, W., Guan, R., Xu, J., 2007. Pentoxifylline attenuates the development of hyperalgesia in a rat model of neuropathic pain. Neurosci. Lett. 412, 268–272.
Lu, C.H., Chao, P.C., Borel, C.O., Yang, C.P., Yeh, C.C., Wong, C.S., Wu, C.T., 2004. Preincisional intravenous pentoxifylline attenuating perioperative cytokine response, reducing

morphine consumption, and improving recovery of bowel function in patients undergoing colorectal cancer surgery. Anesth. Analg. 99, 1465–1471.
Lundblad, R., Ekstrom, P., Giercksky, K.E., 1995. Pentoxifylline improves survival and reduces tumor necrosis factor, interleukin-6, and endothelin-1 in fulminant intra-abdominal sepsis in rats. Shock 3, 210–215.
Ma, W., Quirion, R., 2002. Partial sciatic nerve ligation induces increase in the phosphorylation of extracellular signal-regulated kinase (ERK) and c-Jun N-terminal kinase (JNK) in astrocytes in the lumbar spinal dorsal horn and the gracile nucleus. Pain 99, 175–184.
Marchand, F., Perretti, M., McMahon, S.B., 2005. Role of the immune system in chronic pain. Nat. Rev. Neurosci. 6, 521–532.
Mika, J., Osikowicz, M., Makuch, W., Przewlocka, B., 2007. Minocycline and pentoxifylline attenuate allodynia and hyperalgesia and potentiate the effects of morphine in rat and mouse models of neuropathic pain. Eur. J. Pharmacol. 560, 142–149.
Mika, J., Wawrzczak-Bargiela, A., Osikowicz, M., Makuch, W., Przewlocka, B., 2009. Attenuation of morphine tolerance by minocycline and pentoxifylline in naive and neuropathic mice. Brain Behav. Immun. 23, 75–84.
Milligan, E.D., Twining, C., Chacur, M., Biedenkapp, J., O'Connor, K., Poole, S., Tracey, K., Martin, D., Maier, S.F., Watkins, L.R., 2003. Spinal glia and proinflammatory cytokines mediate mirror-image neuropathic pain in rats. J. Neurosci. 23, 1026–1040.
Mishra, M.K., Ghosh, D., Duseja, R., Basu, A., 2009. Antioxidant potential of Minocycline in Japanese encephalitis virus infection in murine neuroblastoma cells: correlation with membrane fluidity and cell death. Neurochem Int. 54, 464–470.
Nakagawa, T., Wakamatsu, K., Zhang, N., Maeda, S., Minami, M., Satoh, M., Kaneko, S., 2007. Intrathecal administration of ATP produces long-lasting allodynia in rats: differential mechanisms in the phase of the induction and maintenance. Neuroscience 147, 445–455.
Narita, M., Yoshida, T., Nakajima, M., 2006. Direct evidence for spinal cord microglia in the development of a neuropathic pain-like state in mice. J. Neurochem. 97, 1337–1348.
Neuner, P., Klosner, G., Schauer, E., Pourmojib, M., Macheiner, W., Grünwald, C., Knobler, R., Schwarz, A., Luger, T.A., Schwarz, T., 1994. Pentoxifylline in vivo down-regulates the release of IL-1 beta, IL-6, IL-8 and tumour necrosis factor-alpha by human peripheral blood mononuclear cells. Immunology 83, 262–267.
Obata, H., Eisenach, J.C., Hussain, H., Bynum, T., Vincler, M., 2006. Spinal glial activation contributes to postoperative mechanical hypersensitivity in the rat. J. Pain 7, 816–822.
Paxinos, G., Watson, C., 1986. The rat brain in stereotaxic coordinates, second ed. Academic Press, New York.
Perry, V.H., Matyszak, M.K., Fearn, S., 1993. Altered antigen expression of microglia in the aged rodent CNS. Glia 7, 60-7. Review.
Popovich, P.G., Wei, P., Stokes, B.T., 1997. Cellular inflammatory response after spinal cord injury in Sprague–Dawley and Lewis rats. J. Comp. Neurol. 377, 443–464.
Qin, M., Wang, J.J., Cao, R., Zhang, H., Duan, L., Gao, B., Xiong, Y.F., Chen, L.W., Rao, Z.R., 2006. The lumbar spinal cord glial cells actively modulate subcutaneous formalin induced hyperalgesia in the rat. Neurosci. Res. 55, 442–450.
Raghavendra, V., Tanga, F., Rutkowski, M.D., DeLeo, J.A., 2003. Anti-hyperalgesic and morphine-sparing actions of propentofylline following peripheral nerve injury in rats: mechanistic implications of spinal glia and proinflammatory cytokines. Pain 104, 655–664.
Raghavendra, V., Tanga, F.Y., DeLeo, J.A., 2004. Complete Freunds adjuvant-induced peripheral inflammation evokes glial activation and proinflammatory cytokine expression in the CNS. Eur. J. Neurosci. 20, 467–473.
Robinson, A.P., White, T.M., Mason, D.W., 1986. Macrophage heterogeneity in the rat as delineated by two monoclonal. Antibodies MRC OX-41 and MRC OX-42, the latter recognizing complement receptor type 3. Immunology 57, 239–247.
Rodriguez Parkitna, J., Korostynski, M., Kaminska-Chowaniec, D., Obara, I., Mika, J., Przewlocka, B., Przewlocki, R., 2006. Comparison of gene expression profiles in neuropathic and inflammatory pain. J. Physiol. Pharmacol. 57, 401–414.
Schafer, M.K., Schwaeble, W.J., Post, C., Salvati, P., Calabresi, M., Sim, R.B., Petry, F., Loos, M., Weihe, E., 2000. Complement C1q is dramatically up-regulated in brain microglia in response to transient global cerebral ischemia. J. Immunol. 164, 5446–5452.
Smith, K., Leyden, J.J., 2005. Safety of doxycycline and minocycline: a systematic review. Clin. Ther. 27, 1329–1342. Review.
Sommer, C., Schafers, M., 1998. Painful mononeuropathy in C57BL/Wld mice with delayed wallerian degeneration:differential effects of cytokine production and nerve regeneration on thermal and mechanical hypersensitivity. Brain Res. 784, 154–162.
Sterling, D.P., Khodarahmi, K., Liu, J., McPhail, L.T., McBride, C.B., Steeves, J.D., Ramer, M.S., Tetzlaff, W., 2004. Minocycline treatment reduces delayed oligodendrocyte death, attenuates axonal dieback, and improves functional outcome after spinal cord injury. J. Neurosci. 24, 2182–2190.
Strassburger, M., Braun, H., Reymann, K.G., 2008. Anti-inflammatory treatment with the p38 mitogen-activated protein kinase inhibitor SB239063 is neuroprotective, decreases the number of activated microglia and facilitates neurogenesis in oxygen-glucose-deprived hippocampal slice cultures. Eur. J. Pharmacol. 592, 55–61.
Sweitzer, S., Martin, D., DeLeo, J.A., 2001. Intrathecal interleukin-1 receptor antagonist in combination with soluble tumor necrosis factor receptor exhibits an anti-allodynic action in a rat model of neuropathic pain. Neuroscience 103, 529–539.
Tanga, F.Y., Raghavendra, V., DeLeo, J.A., 2004. Quantitative real-time RT-PCR assessment of spinal microglial and astrocytic activation markers in a rat model of neuropathic pain. Neurochem. Int. 45, 397–407.
Tawfik, V., DeLeo, J.A., 2007. Modulating glial activation in opioid tolerance and neuropathic pain: a role for glutamate transporters. In: DeLeo, J.A., Sorkin, L.S., Watkins, L.R. (Eds.), Immune and glial regulation of pain. IASP Press, pp. 341–361.
Temburni, M.K., Jacob, M.H., 2001. New functions for glia in the brain. Proc. Natl. Acad. Sci. U. S. A. 98, 3631–3642.
Tikka, T., Fiebich, B.L., Goldsteins, G., Keinanen, R., Koistinaho, J., 2001. Minocycline, a tetracycline derivative, is neuroprotective against excitotoxicity by inhibiting activation and proliferation of microglia. J. Neurosci. 21, 2580–2588.
Watkins, L.R., Maier, S.F., 2003. Glia: a novel drug discovery target for clinical pain. Nat. Rev. Drug Discov. 2, 973–985.
Watkins, L.R., Milligan, E.D., Maier, S.F., 2001. Spinal cord glia: new players in pain. Pain 93, 201–205.
Watkins, R., Hutchinson, M.R., Johnston, I.N., Maier, S.F., 2005. Glia: novel counter-regulators of opioid analgesia. Trends Neurosci. 28, 661–669.
Wie, T., Sabsovich, I., Guo, T.Z., Shi, X., Zhao, R., Li, W., Geis, C., Sommer, C., Kingery, W.S., Clark, D.J., 2009. Pentoxifylline attenuates nociceptive sensitization and cytokine expression in a tibia fracture rat model of complex regional pain syndrome. Eur. J. Pain 13, 253–262.
Willoughby, J.O., Mackenzie, L., Broberg, M., Thoren, A.E., Medvedev, A., Sims, N.R., Nilsson, M., 2003. Fluorocitrate-mediated astroglial dysfunction causes seizures. J Neurosci. Res. 74, 160–166.
Wordliczek, J., Szczepanik, A.M., Banach, M., Turchan, J., Zembala, M., Siedlar, M., Przewlocki, R., Serednicki, W., Przewlocka, B., 2000. The effect of pentoxifylline on post-injury hyperalgesia in rats and postoperative pain in patients. Life Sci. 66, 1155–1164.
Xin, W.J., Weng, H.R., Dougherty, P.M., 2009. Plasticity in expression of the glutamate transporters GLT-1 and GLAST in spinal dorsal horn glial cells following partial sciatic nerve ligation. Molecular Pain 26, 5–15.
Xu, J.T., Xin, W.J., Wei, X.H., Wu, C.Y., Ge, Y.X., Liu, Y.L., Zang, Y., Zhang, T., Li, Y.Y., Liu, X.G., 2007a. p38 activation in uninjured primary afferent neurons and in spinal microglia contributes to the development of neuropathic pain induced by selective motor fiber injury. Exp. Neurol. 204, 355–365.
Xu, M., Bruchas, M.R., Ippolito, D.I., Gendron, L., Chavkin, C., 2007b. Sciatic Nerve Ligation-Induced Proliferation of Spinal Cord Astrocytes Is Mediated by kappa Opioid Activation of p38 Mitogen-Activated Protein Kinase. J. Neurosci. 27, 2570–2581.
Yong, V.W., Wells, J., Giuliani, F., Casha, S., Power, C., Metz, L.M., 2004. The promise of minocycline in neurology. Lancet Neurol. 3, 744–751.
Yrjänheikki, J., Tikka, T., Keinänen, R., Goldsteins, G., Chan, P.H., Koistinaho, J., 1999. A tetracycline. derivative, minocycline, reduces inflammation and protects against focal cerebral ischemia with a wide therapeutic window. Proc. Natl. Acad. Sci. U.S.A. 96, 13496–13500.
Zabel, P., Schade, F.U., Schlaak, M., 1993. Inhibition of endogenous TNF formation by pentoxifylline. Immunobiology 187, 447–463.
Zhang, L., Shirayama, Y., Shimizu, E., Iyo, M., Hashimoto, K., 2006. Protective effects of minocycline on 3, 4-methylenedioxymethamphetamine-induced neurotoxicity in serotonergic and dopaminergic neurons of mouse brain. Eur. J. Pharmacol. 544, 1–9.
Zimmermann, M., 1983. Ethical guidelines for investigations of experimental pain in conscious animals. Pain 16, 109–110.
Zimmermann, M., 2001. Pathobiology of neuropathic pain. Eur. J. Pharmacol. 429, 23–37.